

## **CAD on Brain, Fundus, and Breast Images**

Hiroshi Fujita<sup>1</sup>, Yoshikazu Uchiyama<sup>1</sup>, Toshiaki Nakagawa<sup>1</sup>, Daisuke Fukuoka<sup>2</sup>,  
Yuji Hatanaka<sup>3</sup>, Takeshi Hara<sup>1</sup>, Yoshinori Hayashi<sup>1</sup>, Yuji Ikedo<sup>1</sup>, Gobert N. Lee<sup>1</sup>,  
Xin Gao<sup>1</sup>, and Xiangrong Zhou<sup>1</sup>

<sup>1</sup>Department of Intelligent Image Information, Division of Regeneration and Advanced  
Medical Sciences, Graduate School of Medicine, Gifu University, Gifu 501-1194, Japan

<sup>2</sup>Faculty of Education, Gifu University, Gifu 501-1193, Japan

<sup>3</sup>Gifu National College of Technology, Motosu City, Gifu 501-0495, Japan  
{fujita@fjt.info.gifu-u.ac.jp}

**Abstract.** Three computer-aided detection (CAD) projects are hosted at the Gifu University, Japan as part of the “Knowledge Cluster Initiative” of the Japanese Government. These projects are regarding the development of CAD systems for the early detection of (1) cerebrovascular diseases using brain MRI and MRA images by detecting lacunar infarcts, unruptured aneurysms, and arterial occlusions; (2) ocular diseases such as glaucoma, diabetic retinopathy, and hypertensive retinopathy using retinal fundus images; and (3) breast cancers using ultrasound 3-D volumetric whole breast data by detecting the breast masses. The brain CAD system achieves a sensitivity of 96.8% at 0.71 false positive (FP) per image for the lacunar-infarct detection, and 93.8% at 1.2 FPs per patient for the small unruptured aneurysm detection. The sensitivity and specificity for the detection of abnormal cases with arterial occlusions in MRA images are 80.0% and 95.3%, respectively. For the glaucoma detection using the retinal fundus CAD system, a sensitivity and specificity of 77.8% and 74.5% are obtained in the analysis of the optic nerve head and a sensitivity of 61.5% at 1.3 FPs per image is achieved in the detection of the retinal nerve fiber layer defects. Hemorrhages and exudates in diabetic retinopathy diagnosis are detected at a sensitivity and specificity of 84.6% and 20.6%, respectively, for the former and 76.9% and 83.3%, respectively, for the latter. For hypertensive retinopathy, the arteriolar-narrowing scheme can identify 76.2% of true positives at 1.4 FPs per image. For the breast CAD system, the image viewer that constructs the breast volume image data is developed, which also includes the CAD function with a sensitivity of 80.5% at 3.8 FPs per breast. The CAD schemes are still being improved for all the systems along with an increase in the number of image databases. Clinical examinations will be started soon, and commercialized CAD systems for the above subjects will appear by the completion of this project.

**Keywords:** Computer-Aided Detection (CAD), Brain MRI, Brain MRA, Cerebrovascular Disease, Lacunar Infarct, Unruptured Aneurysm, Arterial Occlusion, Retinal Fundus Image, Glaucoma, Diabetic Retinopathy, Hypertensive Retinopathy, Ultrasound Breast Images, Breast Cancer

## **1 Introduction**

Since 2002, eighteen knowledge clusters have been established in Japan under the “Knowledge Cluster Initiative” of the Japanese Government. These clusters are supported by the Ministry of Education, Culture, Sports, Science and Technology of Japan under a Grant-In-Aid for Scientific Research with a budget of USD 4.5 million per year per cluster over five years. The aim of the clusters is to promote industrial, academic and governmental cooperation in regional areas and to conduct innovative and technological research with a focus on the needs of industry. The clusters are based in universities and other research institutes in order to draw sources of advanced knowledge; hence, the name “knowledge cluster.”

The Fujita Laboratory at Gifu University is part of the Gifu/Ogaki Robotics Advanced Medical Cluster with a focus on research in distinctive, new medical technologies and developing the state-of-the-art medical equipments such as surgery robots and medical diagnosis support equipments. Currently, there are three established cluster projects in the Fujita Laboratory, Gifu University, started since April 2004. These three projects are computer-aided detection (CAD) systems using brain magnetic resonance imaging (MRI) and magnetic resonance angiography (MRA) images, retinal fundus images and ultrasound breast images, and are described in the following sections.

## **2 CAD for MR Brain Images**

### **2.1 Overview**

Cerebrovascular disease is the third leading cause of death by disease in Japan [1]. Therefore, the screening system, which is named *Brain Dock*, has been widely used for the detection of asymptomatic brain diseases. The prevention of this disease is of paramount importance. MRI and MRA are very useful for the early detection of cerebral and cerebrovascular diseases. Lacunar infarcts, unruptured aneurysms, and arterial occlusions can be detected using MRI and MRA. These medical conditions indicate an increased risk of severe cerebral and cerebrovascular diseases. The presence of lacunar infarcts increases the risk of serious cerebral infarction, and a ruptured aneurysm is the major cause of subarachnoid haemorrhage (SAH).

It is important to detect lacunar infarcts, unruptured aneurysms, and arterial occlusions. However, visualization of these structures is not always easy for radiologists and neurosurgeons. For example, it is difficult to distinguish between lacunar infarcts and normal tissue such as Virchow-Robin spaces in MRI images. Small aneurysms in MRA studies are also difficult to distinguish from the adjacent vessels in a maximum intensity projection (MIP) image. CAD systems can assist

neuroradiologists and general radiologists in detecting intracranial aneurysms, asymptomatic lacunar infarcts, and arterial occlusions and in assessing the risk of cerebral and cerebrovascular diseases. In this project, we use T1- and T2-weighted MRI brain images for the detection of asymptomatic lacunar infarcts [2, 3]. We also employ MRA brain images for the detection of intracranial aneurysms [4] and for developing a new viewing technique to facilitate the detection of intracranial aneurysms [5] and arterial occlusions [6].

## 2.2 Detection of Lacunar Infarct

The CAD scheme for detecting lacunar infarcts in MRI is shown in Figure 1. The cerebral region is first extracted from a T1-weighted image. Lacunar infarct candidates are extracted using a simple thresholding technique and a top-hat transformation on T2-weighted images. Twelve features are measured from each candidate and a neural network is used in the final classification of the lacunar infarcts [2, 3]. Using the above procedure for detecting lacunar infarcts, our developed CAD scheme can achieve a sensitivity of 96.8% at 0.71 false positive (FP) per image in a dataset of 132 studies.

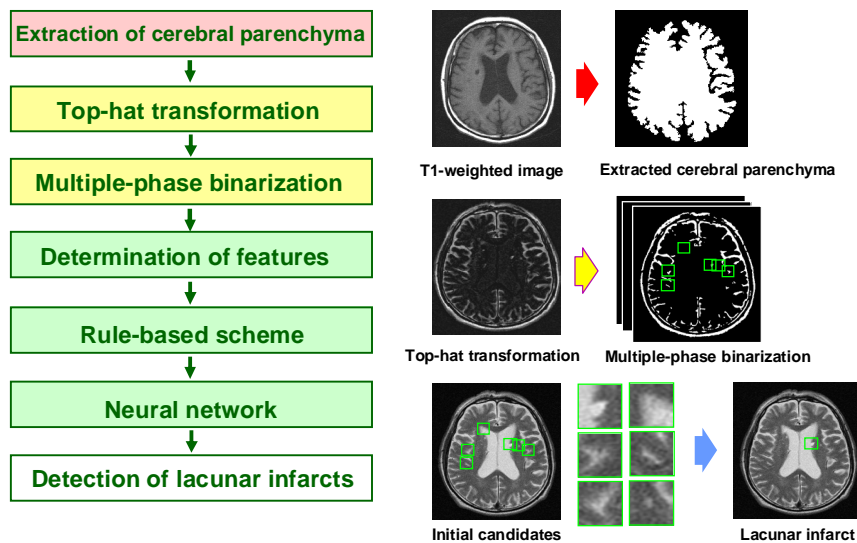


**Fig. 1.** Overall CAD scheme for the detection of lacunar infarcts [3]. Initial candidates are found in the three steps of image processing and then the FPs are reduced using the feature analysis of rule-based and neural-network techniques. The lacunar infarct(s) finally detected is marked with a small square on the T2-weighted image, in which it appears as tiny round-shaped object with a “white” color, as shown in the bottom-right image.

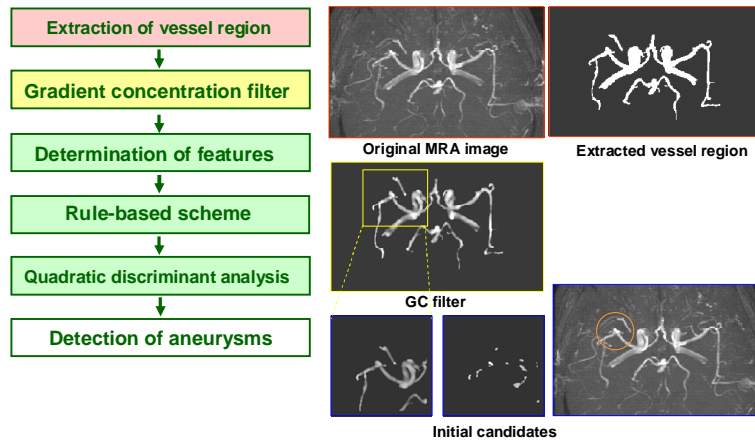


**Fig. 2.** Overall CAD scheme for the detection of aneurysms [4, 5]. Initial candidates are determined in the gradient concentration image using a threshold. Rule-based schemes and quadratic discriminant analysis are employed for distinguishing between aneurysms and FPs. An unruptured aneurysm is detected and is marked on the MIP image with a circle in the bottom-right image.

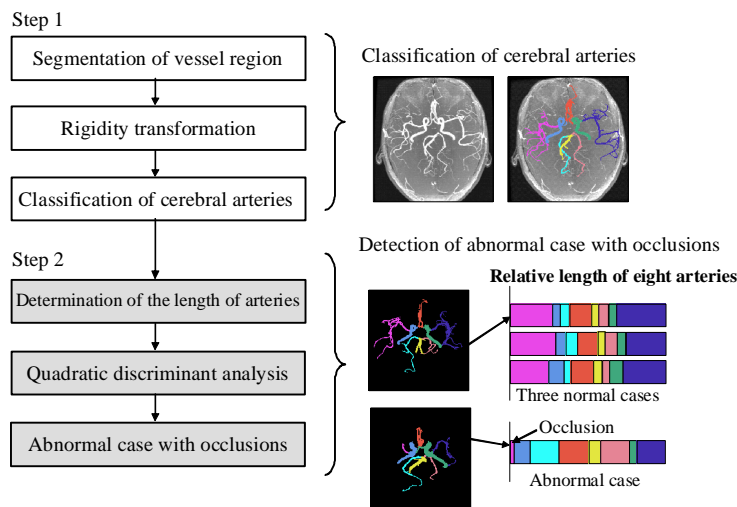


**Fig. 3.** Our scheme for automated detection of arterial occlusions comprises two parts, i.e., (1) classification of eight arteries, and (2) detection of occlusions based on the relative lengths of eight arteries [6]. For the classification of arteries, the segmented vessel regions are classified into eight arteries based on a comparison of the target image with a reference image. For the detection of an arterial occlusion, a classifier that uses the relative lengths of the arteries as features is employed in distinguishing between the normal cases and the abnormal cases with arterial occlusions.

### **2.3 Detection of Unruptured Aneurysm**

The overall scheme for the detection of unruptured aneurysm is shown in Figure 2. Vessel regions are first extracted from MRA images using linear gray-level transformation. A gradient concentration filter is then used to enhance the candidate aneurysms and quadratic discriminant analysis is used for the final detection of aneurysms [4, 5]. In a dataset of 100 MRA studies, our current CAD scheme achieves a sensitivity of 93.8% at an FP detection of 1.2 per patient.

### **2.4 Detection of Occlusion**

The overall scheme for the detection of arterial occlusion in MRA studies is shown in Figure 3, in which the scheme consists of two parts, i.e., (1) classification of eight arteries based on the comparison of the target image with the reference image, and (2) detection of arterial occlusion(s) based on the relative lengths of eight arteries [6]. The sensitivity and specificity for the detection of abnormal cases with arterial occlusions are 80.0% and 95.3%, respectively, for the cases of 100 MRA studies including 15 arterial occlusions.

## **3 CAD for Retinal Fundus Images**

### **3.1 Overview**

Retinal fundus images are useful for the early detection of a number of ocular diseases—if left untreated, can lead to blindness. Examinations using retinal fundus images are cost effective and are suitable for mass screening. In view of this, retinal fundus images are obtained in many health care centers and medical facilities during medical checkups for ophthalmic examinations. Figure 4 depicts the fundus images with glaucoma, diabetic retinopathy, and hypertensive retinopathy, which are targeted in this project. The increase in the number of ophthalmic examinations improves ocular health care in the population but it also increases the workload of ophthalmologists. Therefore, CAD systems developed for analyzing retinal fundus images can assist in reducing the workload of ophthalmologists and improving the screening accuracy.

### **3.2 Detection of Glaucoma**

In a population-based prevalence survey of glaucoma in Tajimi City, Japan, one in 20 people who are aged over 40 was diagnosed with glaucoma [7, 8]. Around the world, the number of people with glaucoma is estimated to be 60.5 million in 2010 and 79.6 million in 2020 [9]. Glaucoma is the second leading cause of blindness in Japan and also worldwide. Although it cannot be cured, glaucoma can be treated if

diagnosed early. Mass screening for glaucoma using retinal fundus images is simple and effective.

In the CAD system developed in this project, two different approaches are used for the detection of glaucoma. The first one is based on the measurement of the cup-to-disc (C/D) ratio. Blood vessels are first “erased” from the fundus image by image processing technique and the optical nerve head is located. The C/D ratio, which is the ratio of the diameter of the depression (cup) and that of the optic nerve head (ONH, i.e., disc), is evaluated for the diagnosis of glaucoma (Figure 5). Using 65 cases (47 normal and 18 abnormal), the sensitivity and specificity are reported at 77.8% and 74.5%, respectively.

We are also developing a method for measuring the depth of the cup by using our new digital stereo fundus camera along with an automatic reconstruction technique [10, 11] in an extended project, as a part of the Regional New Consortium Projects from Ministry of Economy, Trade and Industry, Japan.

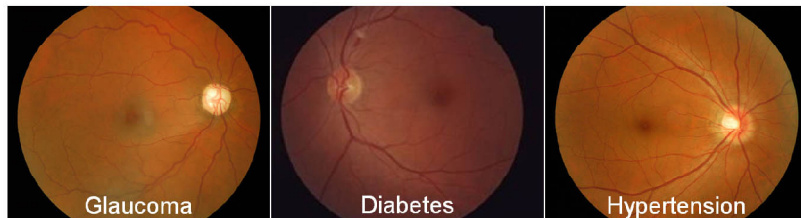


**Fig. 4.** Retinal fundus images showing glaucoma, diabetes, and hypertension.

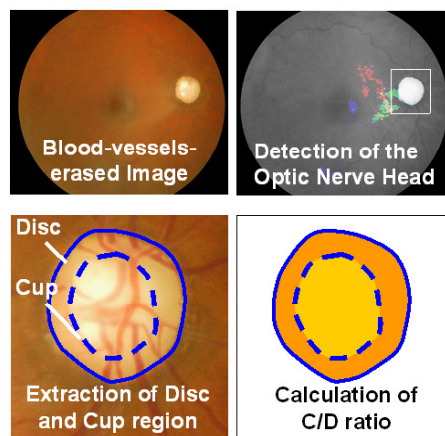


**Fig. 5.** Determination of the C/D ratio for the diagnosis of glaucoma. (Left to right; top to bottom) Blood vessels are first “erased” from the original image and the optic nerve head is located. A fundus image with a C/D ratio greater than 0.60 is considered to be abnormal.

The second approach developed in this project for the diagnosis of glaucoma is based on the detection of retinal nerve fiber layer defects (NFLDs) using image processing techniques [12]. Blood vessels in the original fundus image are erased and the optic disc is located as described previously. The fundus image is then transformed into a rectangular array before enhancing the NFLDs with Gabor filtering (Figure 6). Using 26 normal and 26 abnormal fundus images with 53 NFLD regions, this approach can identify 61.5% of true positives at 1.3 FPs per image.

### **3.3 Detection of Diabetic Retinopathy**

In Japan, the number of people with adult diseases such as diabetes and hypertension is increasing every year. Diabetic retinopathy is the leading cause of blindness in Japan; this is a complication associated with diabetes. The probability for diabetic patients developing diabetic retinopathy within 10 years of the onset of diabetes is high. To prevent this disease, people aged over 40 or those who are at a risk should attend mass screening or have regular eye examinations. In an ophthalmologic examination, ophthalmologists look for the presence of hemorrhages (including microaneurysms) and exudates in the retinal fundus images.

Figures 7 and 8 show the detection schemes developed for hemorrhages and exudates, respectively. For hemorrhage detection, the initial extraction includes both the hemorrhages and blood vessels. The blood vessels are subsequently identified and eliminated. In addition, the funicular shapes included in the initial extraction are also identified and eliminated. Further FP elimination is performed using feature analysis. A similar procedure is used in the exudates detection [13].

Using 113 fundus images (26 with hemorrhages and 87 normal), the sensitivity and specificity of the hemorrhage detection algorithm was evaluated to be 84.6% and 20.6%, respectively. Using 109 fundus images (13 with exudates and 96 normal), the sensitivity and specificity of the exudates detection algorithm was evaluated at 76.9% and 83.3%, respectively.

### **3.4 Detection of Hypertensive Retinopathy**

Hypertensive retinopathy can also benefit from the analysis of retinal fundus images. With severe hypertensive retinopathy, the damage to the optic nerve or macula can be permanent. Figure 9 shows the hypertensive retinopathy detection scheme based on the measurement of the vascular diameter [14]. Our scheme comprises the extraction of blood vessels, classification of arteries and veins, and detection of arteriolar narrowing by the artery-vein diameter ratio (A/V ratio). An A/V ratio  $>0.67$  is considered as abnormal. Using 39 normal and 44 abnormal fundus images with arteriolar narrowing, this approach can identify 76.2% of true positives at 1.4 FPs per image.

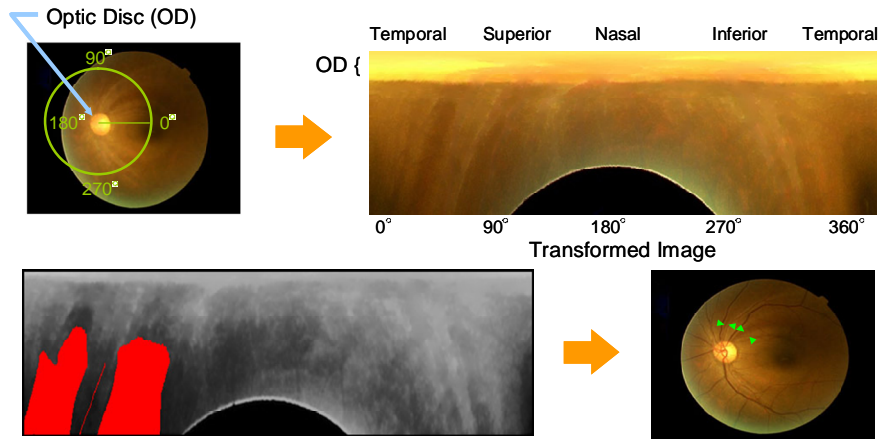


**Fig. 6.** Detection of NFLDs using Gabor filtering [12]. (Top: left to right) Centered at the optic disc, the fundus image is transformed into a rectangular array by reading out the pixel values using polar coordinates. (Bottom: left to right) Gabor filtering is applied to the transformed image. The NFLD regions are enhanced and the candidates are indicated in red. After the elimination of FPs, the rectangular array is back-transformed and the detected NFLDs are marked using pairs of green arrows.

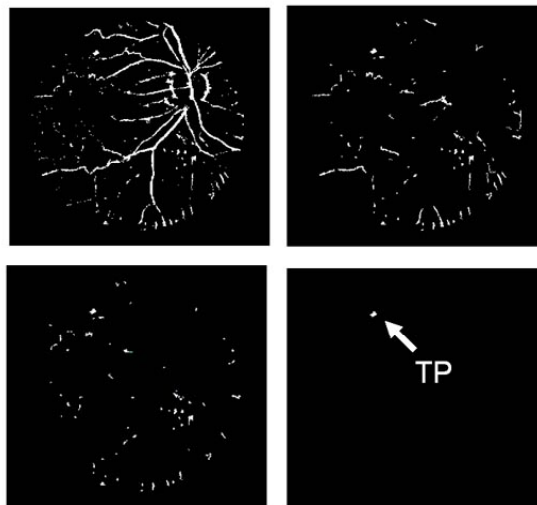


**Fig. 7.** Detection of hemorrhages [13]. (Left to right, top to bottom) Initial extraction of hemorrhages with blood vessels; blood vessels are identified and erased; elimination of funicular shape regions; elimination of FPs using feature analysis. TP denotes true positive detection.



**Fig. 8.** Detection of exudates [13]. (Left to right, top to bottom) Original retinal fundus image; initial detection of exudates; FPs reduction using shape analysis; FPs reduction using feature analysis. TP denotes true positive detection.

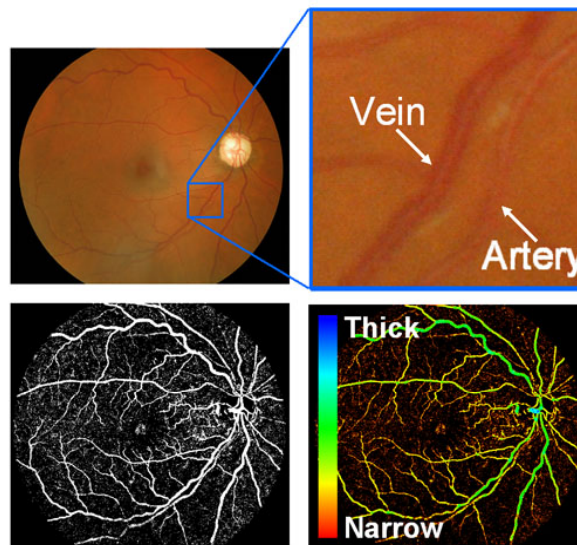


**Fig. 9.** Detection scheme of hypertensive retinopathy [14]. (Left to right, top to bottom) Original retinal fundus image; magnified view showing the difference in the diameter between a vein and an artery; extraction of blood vessels; the ratio of the size of the artery to that of the vein (A/V ratio) is determined. An A/V ratio  $>0.67$  is considered as abnormal.

## 4 CAD for Ultrasound Breast Images

### 4.1 Overview

In Japan, breast cancer has the highest incidence rate among all the cancers in women [15]. It is also one of the most common causes of cancer death for women in many Western countries. Early detection of breast cancer is the key to simpler treatment and a better prognosis. In view of this, many countries, including Japan have introduced breast cancer screening programs. Mammography is widely used in breast cancer screening. Its effectiveness in detecting breast cancer in women aged over 50, typically with less dense breast tissues, has been established. However, mammography is less effective for younger women or women with dense breast tissues.

In Japan, women typically have denser breast tissues than their counterparts in Western countries. Consequently, the image contrast between cancerous breast mass tissues and the dense breast tissues in mammographic images is low; thus, the detection of breast cancer over a background of dense breast tissue is difficult. Ultrasonography, on the other hand, is effective in distinguishing and characterizing breast masses set in a dense-breast-tissue environment. Currently, breast ultrasound is primarily used for the diagnosis of breast cancer, as opposed to the screening of breast cancer. There is a growing need for ultrasound examination to be available for breast cancer screening in women with dense breast tissues.



**Fig. 10.** An overall system for breast cancer screening using ultrasound images. The system consists of an ultrasound imaging device and a whole breast scanning device for whole breast volumetric data acquisition. A workstation is also included for the purpose of pre-processing and analysis of the images acquired by the scanning device from the patient and as a viewer for the visualization of the images along with the CAD results [16].

#### 4.2 Whole Breast Scanner and CAD

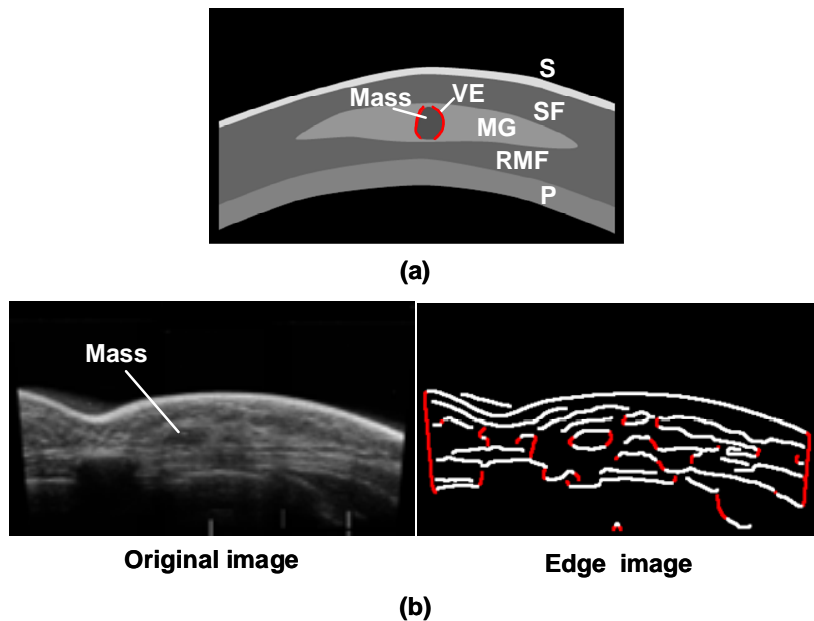
Current diagnostic ultrasound breast images are obtained using conventional hand-held probes. Here, the results of the examinations are operator dependent and the reproducibility is poor. Moreover, the procedure is lengthy if the whole breast is to be scanned.

Figure 10 shows our system developed for breast cancer screening using ultrasound images. An automatic whole-breast scanner (ASU-1004, Aloka Co. Ltd, Japan) is used in acquiring and screening breast images. The scanner is an automated water path system and can scan the whole breast in sweeps. A 3D volumetric whole breast data is reconstructed from the original scans in the workstation, which has a capability of the image viewer with CAD function [16] (Figure 11).

Using a Canny's detector, the edge information in the ultrasound images is enhanced and analyzed (Figure 12). Normal structures in breast ultrasound images typically do not contain vertical edges. The detection of vertical edges in the image suggests abnormal structures [16]. Using 109 whole-breast ultrasound patient cases, our CAD system for breast-mass detection achieves a sensitivity of 80.5% at 3.8 FPs per breast. A CAD system that uses a bilateral subtraction technique to reduce the FPs detected by the mass detection scheme has also been developed [17]. It was found that a scheme for FP reduction based on the bilateral subtraction technique can effectively reduce FPs because 67.3% of the FPs was reduced without removing a true positive region.



**Fig. 11.** The 3D whole-breast volumetric data is constructed by “stitching” together the images from the three sweeps (only one slice is shown) [16].



**Fig. 12.** Illustration of the detection of a low-echo breast mass. (a) Schematic diagram of structures in a breast ultrasound image where S is skin layer, SF is subcutaneous fat, MG is mammary gland, RMF is the retro-mammary fat, P is pectorals and VE is a near-vertical edge of the mass. (b) The original breast ultrasound image and the processed edge image are shown [16].

\*\*\*

In summary, all of the CAD projects are proceeding very well thus far and the clinical examinations will be started soon; according to our plan, commercialized CAD systems in the field of brain MR images, fundus images, and breast ultrasound images will appear by the completion of this project (March 2009).

**Acknowledgements.** The studies described above are supported mainly by a grant for the Knowledge Cluster Gifu-Ogaki (KCGO), referred to as the “Robotics Advanced Medical Cluster,” from the Ministry of Education, Culture, Sports, Science and Technology, Japan, and also in part by a grant for Regional New Consortium Projects from the Ministry of Economy, Trade and Industry, Japan. The authors are grateful to their many co-workers from universities, hospitals, and companies (TAK Co., Ltd., Konica Minolta Medical & Graphics, Inc., Kowa Co., Ltd., and Aloka Co., Ltd., Japan) who are involved in the “Big CAD projects” at KCGO.

## References

1. Health and Welfare Statistics Association: Vital Statistics of Japan 2003. 1 (2003) 300-301
2. Yokoyama, R., Zhang, X., Uchiyama, Y., Fujita, H., Hara, T., Zhou, X., Kanematsu, M., Asano, T., Kondo, H., Goshima, S., Hoshi, H., Iwama, T.: Development of an Automated Method for the Detection of Chronic Lacunar Infarct Regions in Brain MR images. IEICE Trans. Inf. & Syst. E90-D (6) (2007) 943-954
3. Uchiyama, Y., Matsui, A., Yokoyama, R., Fujita, H., Hara, T., Zhou, X., Ando, H., Iwama, T., Asano, T., Kato, H., Hoshi, H.: CAD Scheme for Detection of Lacunar Infarcts in Brain MR Images. International J. of Computer Assisted Radiology and Surgery 1 Supplement 1 (2006) 382-385
4. Uchiyama, Y., Ando, H., Yokoyama, R., Hara, T., Fujita, H., Iwama, T.: Computer-Aided Diagnosis Scheme for Detection of Unruptured Intracranial Aneurysms in MR Angiography. Proc. of IEEE Engineering in Medicine and Biology 27th Annual Conference, Shanghai, China, (2005), 3031-3034
5. Uchiyama, Y., Yamauchi, M., Ando, H., Yokoyama, R., Hara, T., Fujita, H., Iwama, T.: Automatic Classification of Cerebral Arteries in MRA Images and Its Application to Maximum Intensity Projection. Proc. of IEEE Engineering in Medicine and Biology 28th Annual Conference, New York, USA, (2006), 4865-4868
6. Yamauchi, M., Uchiyama, Y., Yokoyama, R., Hara, T., Fujita, H., Ando, H., Yamakawa, H., Iwama, T., Hoshi, H.: Computerized Scheme for Detection of Arterial Occlusion in Brain MRA images. Proc. of SPIE Medical Imaging 2007: Computer-Aided Diagnosis Vol. 6514 (2007) 65142C-1-65142C-9
7. Iwase, A., Suzuki, Y., Araie, M., et al. and Tajimi Study Group, Japan Glaucoma Society: The Prevalence of Primary Open-angle Glaucoma in Japanese The Tajimi Study. Ophthalmology 111 (9) (2004) 1641-1648
8. Yamamoto, T., Iwase, A., Araie, M., and Tajimi Study Group, Japan Glaucoma Society: The Tajimi Study Report 2: Prevalence of Primary Angle Closure and Secondary Glaucoma in a Japanese Population. Ophthalmology 112 (10) (2005) 1661-1669
9. Quigley, H. and Broman, A.: The Number of People with Glaucoma Worldwide in 2010 and 2020. Br. J. Ophthalmol. 90 (2006) 262-267
10. Nakagawa, T., Hayashi, Y., Hatanaka, Y., Aoyama, A., Hara, T., Kakogawa, M., Fujita, H., Yamamoto, T.: Comparison of the Depth of an Optic Nerve Head Obtained using Stereo Retinal Images and HRT. Proc. of SPIE Medical Imaging 2007: Physiology, Function, and Structure from Medical Images Vol. 6511 (2007) 65112M-1-65112M-9
11. Nakagawa, T., Hayashi, Y., Hatanaka, Y., Aoyama, A., Hara, T., Kakogawa, M., Fujita, H., Yamamoto, T.: Cup Region Extraction of Optic Nerve Head for Three-Dimensional Retinal Fundus Image. Proc. of Asian Forum on Medical Imaging, IEICE Technical Report 106 (510) (2007) 26-27

12. Hayashi, Y., Nakagawa, T., Hatanaka, Y., Aoyama, A., Kakogawa, M., Hara, T., Fujita, H., Yamamoto, T.: Detection of Retinal Nerve Fiber Layer Defects in Retinal Fundus Images using Gabor Filtering. Proc. of SPIE Medical Imaging 2007: Computer-Aided Diagnosis Vol. 6514 (2007) 65142Z-1-65142Z-8
13. Hatanaka, Y., Nakagawa, T., Hayashi, Y., Fujita, A., Kakogawa, M., Kawase, K., Hara, T., Fujita, H.: CAD Scheme to Detect Hemorrhages and Exudates in Ocular Fundus Images. Proc. of SPIE Medical Imaging 2007: Computer-Aided Diagnosis Vol. 6514 (2007) 65142M-1-65142M-8
14. Hayashi, T., Nakagawa, T., Hatanaka, Y., Hayashi, Y., Aoyama, A., Mizukusa, Y., Fujita, A., Kakogawa, M., Hara, T., Fujita, H.: An Artery-vein Classification Using Top-hat Image and Detection of Arteriolar Narrowing on Retinal Images. IEICE Technical Report 107 (57) (2007) 127-132 [in Japanese]
15. Minami, Y., Tsubono, Y., Nishino, Y., Ohuchi, N., Shibuya, D., Hisamichi, S.: The Increase of Female Breast Cancer Incidence in Japan: Emergence of Birth Cohort Effect. Int. J. Cancer 108 (6) (2004) 901-906
16. Ikedo, Y., Fukuoka, D., Hara, T., Fujita, H., Takada, E., Endo, T., Morita, T.: Computer-aided Detection System of Breast Masses on Ultrasound Images. Proc. of SPIE Medical Imaging 2006: Image Processing Vol. 6144 (2006) 61445L-1-61445L-8
17. Ikedo, Y., Fukuoka, D., Hara, T., T., Fujita, H., Takada, E., Endo, T., Morita, T.: Computerized mass detection in whole breast ultrasound images: Reduction of false positives using bilateral subtraction technique. Proc. of SPIE Medical Imaging 2007: Computer-Aided Diagnosis Vol. 6514 (2007) 65141T-1-65141T-10